Beach adaptation to intraseasonal sea level changes

G O Abessolo, R Almar, J Jouanno, F Bonou, B Castelle, M Larson

Beach adaptation to intraseasonal sea level changes

Environmental Research Communications

LETTER

Beach adaptation to intraseasonal sea level changes

G O Abessolo[1,2], R Almar[1], J Jouanno[1], F Bonou[3,4], B Castelle[5] and M Larson[6]

[1] LEGOS, OMP, UMR 5566 (CNES-CNRS-IRD-University of Toulouse), Toulouse, France
[2] Ecosystems and Fishery Resources Laboratory, University of Douala, BP 2701 Douala, Cameroon
[3] Laboratoire d'Hydrologie Marine et Côtière, Institut de Recherche Halieutique et Océanologique du Benin (LHMC-IRHOB), Cotonou, Benin
[4] Université Nationale des Sciences, Technologie, Ingénierie et Mathématiques (UNSTIM) Abomey, Benin
[5] EPOC, OASU, UMR 5805 (CNRS-University of Bordeaux), Pessac, France
[6] Water Resources Engineering, Lund University, Box 118, 22100 Lund, Sweden

E-mail: gregsolo55@yahoo.fr

OPEN ACCESS

RECEIVED
17 October 2019

REVISED
25 March 2020

ACCEPTED FOR PUBLICATION
6 April 2020

PUBLISHED
1 May 2020

Keywords: intra-seasonal time scale, sea level, beach profile, video imagery, altimetry, nearshore, waves

Supplementary material for this article is available online

Abstract

Coastal areas such as beaches with steep upper slope and flat low-tide terrace, are expected to be increasingly affected by sea level changes. Related impacts due to the paramount rise in sea level have been intensively investigated, but there is still little evidence of the impact of shorter timescales variations on the coast, particularly those induced by trapped coastal waves. Using the latest advances in video bathymetric estimation, daily observations over 3.5 years (February 2013 to June 2016) on Grand Popo Beach (West Africa) reveal that intraseasonal sea level variations impact the beach profile. The intraseasonal sea level variations are dominated by the propagation of wind forced coastal trapped waves with periods ranging 15–95 days. It is shown that the beach goes through a transient state with a deformation of the profile: an intraseasonal sea level rise leads to a 2 m erosion of the upper beach and a widening of the flat terrace at the lower beach. Although the underlying mechanism must be tested through beach profile modelling, this study highlights the active adaptation of the beach profile to variations in sea level.

1. Introduction

Most of the world's coasts are subject to changes because of their vulnerability to climate change as well as human development. Climate change drives variations in mean sea level, wave conditions, storm surge, that result in the destruction of socio-economical and environmental systems (Stive *et al* 2002, Rueda *et al* 2017). Understanding the factors responsible for beach erosion and flooding has become a main concern. There is a need to assess and evaluate the trends under present climate conditions, which will be fundamental for predicting future impacts (McInnes *et al* 2016) and for developing effective management policies (Leonard *et al* 2014).

Global seal-level rise is well known to lead to a recession of the shoreline (Bruun 1954, 1962, 1983, 1988, Ranasinghe *et al* 2012, Rosati *et al* 2013, Shand *et al* 2013, Dean and Houston 2016, Le Cozannet *et al* 2016, Atkinson *et al* 2018). It is an important contributor to erosion hotspots at decadal to centenary scales (Zhang *et al* 2004, Nicholls and Cazenave 2010, Passeri *et al* 2014, Le Cozannet *et al* 2019). Conventionally, it is thought that at shorter time scales, from hours to years, waves, tides, sedimentary processes, and anthropogenic factors drive beach changes that surpass sea level impact (Stive 2004, Ranasinghe 2016, Anthony *et al* 2019). This is relevant at mid-to-high latitudes where storm-induced coastal dynamics is dominant. However, this can be different in the inter-tropical band where sea level presents large fluctuations at seasonal and interannual scales (Komar and Enfield 1987, Feng *et al* 2003, Ding *et al* 2009, Pattiaratchi and Eliot 2009, Komar *et al* 2011), and intraseasonal scales (Polo *et al* 2008, Echevin *et al* 2014, Ezer 2016, Ding *et al* 2018, Kim *et al* 2018). While the seasonal and

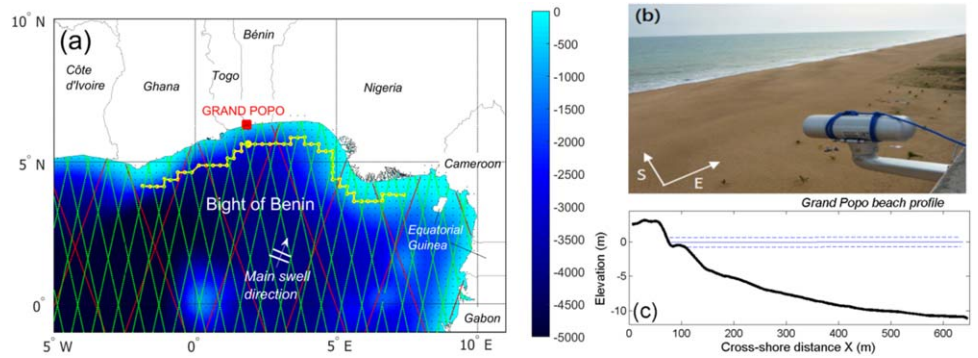

Figure 1. Study site. (a) Bight of Benin, West Africa, Gulf of Guinea. Yellow points stand for selected nodes along the coast used to track propagating sea level variations. Black dots stand for SSALTO/DUACS grid nodes. The tracks of the satellite missions merged in the SSALTO/DUACS gridded product used for the altimetric sea level are indicated: in red for Jason-3 and in green for Saral/Altika. The Cryosat-2 mission is non-sun-synchronous (Wingham *et al* 2006) and moves along drifting tracks (92°-orbit inclinaison) that have not been shown. The color bar gives the bathymetry in meters (GEBCO gridded bathymetry data). Node 34 (5.6271 °N, 1.6375 °E) is the closest point to Grand Popo. (b) Video camera system deployed on a tower made available by the Beninese Navy at Grand Popo. (c) Average beach profile (solid black line) obtained during the Grand Popo experiment (March 10 to 19, 2014), with mean sea level (solid blue line) and high and low (blue dashed blue lines) tide levels. Bathymetric iso-contours are reasonably uniform alongshore.

interannual scales are related to the tropical climate modes, the intraseasonal variability is characterized by the poleward propagation of coastal disturbances triggered by coastally-trapped Kelvin and Rossby waves. These coastally-trapped waves can be caused by wind stress variability, atmospheric disturbances and variations in the intensity of oceanic currents. For instance, Kelvin waves have been intensively described in the equatorial Atlantic and in the equatorial Pacific. Echevin *et al* (2014) reported ±0.20 m of intraseasonal sea level variations on the nearshore Peru ecosystem, within the 60–120 day time periods. At 15°N on the western coast of India, ±0.25 m intraseasonal variations of alongshore currents were observed in the 55–110 day time periods (Vialard *et al* 2009). In West Africa, Gulf of Guinea, Polo *et al* (2008) observed recurrent and continuous wave propagations distinguishable over thousands of kilometers poleward along the coast, in the period range 20–90 days. The observed characteristics were close to those of equatorial Kelvin wave propagations with a variance of 0.02 m and a phase speed ranging from 1.5 to 2.1 m s^{-1} without any substantial differences and no remarkable property changes following the coastline along different isobaths (200 to 1000 m-depth).

Such transient sea-level changes may actually play a part in beach variability (Komar and Enfield 1987). But, how they operate in the coastal zone is still a scientific issue (McInnes *et al* 2016). Segura *et al* (2018) investigated such dynamics at a reef-fringed beach at seasonal scale. Their results suggested that, contrary to general observation on open beaches, the seasonal beach response is primarily influenced by seasonal variations in offshore water level rather than by wave heights. However, this result is specific to reef-fringed beaches. At intraseasonal scale, there is still very little knowledge about the impact of sea levels on the beach, as little attention has been given to it. We hypothesize that intraseasonal sea level variability could drive beach changes, in particular for storm-free and tropical environments, where these intraseasonal sea level changes were reported to be large. However, the lack of suitable measurements and the historical cloisoning of the nearshore and coastal oceanography communities have led to a knowledge gap on transient sea level change impacts. Here we combine regional observation of coastal sea level from satellite altimetry with local scale beach evolution from shore-based video to investigate the nearshore response to intraseasonal sea level variations in the Gulf of Guinea.

2. Study site

This study focuses on beach changes at Grand Popo (Benin) near the border with Togo, in the Bight of Benin, Gulf of Guinea (figure 1). According to the classification of Wright and Short (1984), Grand Popo beach is an intermediate to reflective beach, characterised by a steep upper slope, an alongshore-uniform flat low-tide terrace (Almar *et al* 2014, Abessolo *et al* 2016, 2017b). Bathymetric iso-contours are reasonably uniform alongshore (Almar *et al* 2014). Grand Popo beach is exposed to intermediate incident waves (annual mean: Hs = 1.36 m; Tp = 9.4 s; S-SW) (Almar *et al* 2015, Giardino *et al* 2018). The wave regime is composed of a dominant long-period swell component originating from mid to high latitudes (45°–60°) in the South Atlantic, and wind seas locally generated in the tropical band (6 °N to 15 °S), prevailing from the SW (Almar *et al* 2015). Tides are semi-diurnal with a tidal range of approximately 0.3 m and 1.8 m for neap and spring tides,

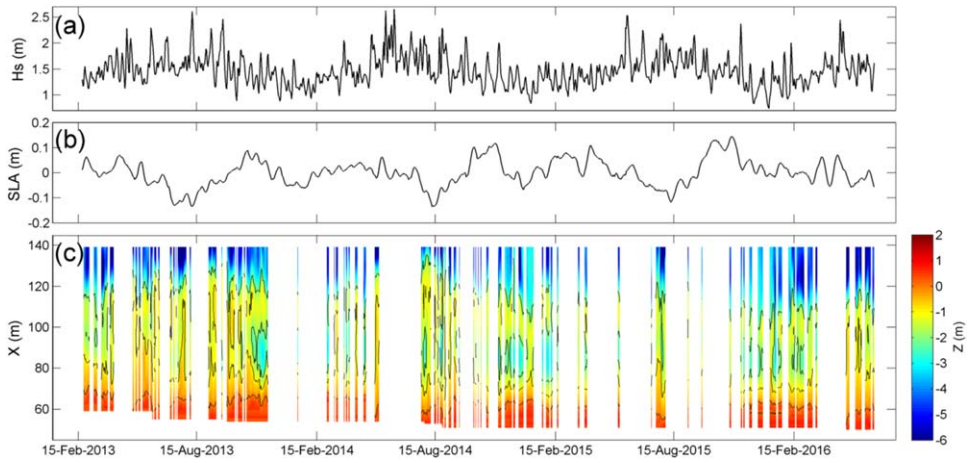

Figure 2. Daily forcing parameters and beach evolution at Grand Popo, Benin: (a) Hs at breaking (using Larson *et al* 2010), (b) SLA (extracted at node 34, see figures 1(a)), and (c) video-derived depths (Z), for the period February 2013 to August 2016. X stands for the cross-shore location from the video camera. Black lines in panel (c) stand for the 0- to 2-m depth contours.

respectively. The sediment size is medium-to-coarse sand, from 0.4 to 1 mm, with a median grain size D50 = 0.6 mm. A seasonal variability of sea level is observed in the Bight of Benin, with fluctuations of approximately 0.2 m, in response to wind-driven basin modes, also involving Kelvin and Rossby wave propagation and reflection (Polo *et al* 2008, Ding *et al* 2009). According to Melet *et al* (2016), the regional trend in sea level rise is 5.1 mm yr^{-1} (over the 20-year period from 1993 to 2013), larger than the global rate.

3. Nearshore bathymetry, ocean waves and sea level data

The first pilot research video station in West Africa was installed in February 2013 on a 20-m high tower located approximately 70 m from the shoreline (Almar *et al* 2014, Abessolo *et al* 2016, 2017a, 2017b). An on-site computer processes the raw image-frames and stores 15-min time stack (Holland and Holman 1993) and timex (Holland *et al* 1997) images. Timex images were obtained by averaging 15 min of snapshots. Time stack images were obtained by stacking the successive traces corresponding to 15 min of snapshots. A single cross-shore track extending approximately 715 m was preset during the installation of the video system and used for this study. The Minimum Shoreline Variability (MSV) method (Almar *et al* 2012) was used to derive alongshore averaged shoreline locations from video timex images. Associated daily intertidal profiles were computed using the method described by Aarninkhof *et al* (2003). Video-based wave celerity and depth inversion schemes (for details, see appendix A is available online at stacks.iop.org/ERC/2/051003/mmedia) were used to derive instant depths from the time stack images. The whole beach profile was derived by merging the daily intertidal and bathymetric profiles. In this paper, the term 'upper beach' will refer to the steepest part of the beach corresponding to the swash zone at high tide, according to Miles and Russel (2004).

A validation of the video-derived beach profiles (Abessolo *et al* 2017a) was conducted for the 10-day field experiment at Grand Popo from March 10 to 19, 2014 (Almar *et al* 2014). Measurements consisted of beach surveys with Differential GPS and bathymetric sonar. The results unveiled the maximum vertical error that was about 0.15 m for the daily depth, along the part of the profile covering the upper beach and the lower part of the terrace ($50 \leqslant X \leqslant 130$ m). The evolution of the beach profile over the 3.5 years of the study period is shown in figure 2. The low-tide terrace is detected at a depth of approximately 1 meter and the width of the terrace is considered as the distance between the shoreline location (0-meter depth contour) and the outer part of the terrace (2 m-depth contour). The observed depth changes suggest that the beach profile varies as follows. The terrace width increases during the winter period (June-July-August) when wave energy is high and decreases during the austral summer period (December-January-February) when wave energy is low. In addition, an erosive trend of -1.6 m yr^{-1} is observed for the upper beach; this trend seems to be even stronger at the end of the terrace (-3.1 m yr^{-1}). Trends were computed as the best linear fit, using the least-squares method.

Wave characteristics (Hs, Tp and direction) were extracted from ERAInterim ECMWF re-analyses (Sterl and Caires 2005) at the node 6.25 °N, 1.73 °E, at 6-hr interval over the study period; the waves were then propagated from deep water to the breakpoint using the formula by Larson *et al* (2010) and averaged daily.

Sea level anomalies (SLA) time series were extracted at daily scale from the SSALTO/DUACS multi-mission gridded and delayed-time products (Amarouche *et al* 2004, Tran *et al* 2010, Arbic *et al* 2012, Pujol *et al* 2016)

provided by Copernicus Marine and Environment Monitoring Service (CMEMS). In these products, available altimeter missions (Saral/AltiKa, Cryosat-2 and OSTM/Jason-2 for the period from 2013 to 2016) are merged and mapped daily onto a 1/4°-resolution grid (Ubelmann *et al* 2015, 2017). In order to identify propagating sea level variations along the coast, data were extracted along a track of 54 grid nodes in the Bight of Benin (see figure 1(a)), close enough to the coast, but not too close to prevent landmasses disturbances in radar signal (see Polo *et al* 2008). The distance between consecutive selected nodes was 1/4° (~27.5 km, according to SSALTO/DUACS grid) and each node was taken approximately 75 km from the coast. Contributions to sea level variations driven by local wind, atmospheric pressure, and waves were neglected, despite their possible importance (Santoro *et al* 2013, Melet *et al* 2016, Slangen *et al* 2017, Melet *et al* 2018). The ocean forcing (Hs and SLA) for the 3.5 years period is shown in figure 2.

4. Intraseasonal sea level forcing

Sea level anomalies along the coast of West and Central Africa observed from altimetry show large variability, with main peaks at the annual, semi-annual, and 120-day period (Polo *et al* 2008, de Coëtlogon *et al* 2010, Jouanno *et al* 2013). The annual and semi-annual components dominate the sea level variability (Aman *et al* 2007). For periods smaller than 100 days, a relative maximum is observed at a 60-day period (Polo *et al* 2008). This temporal band corresponds to coastal trapped waves that propagate from the equator north to Senegal, and whose properties resemble that of a pure coastal Kelvin wave in the limit where the continental margin tends to zero. The study by Polo *et al* (2008) used Topex/Poseidon products at 7-day time resolution and retained the range 25–95 day for detecting these intraseasonal waves. Here, the use of SSALTO/DUACS products with daily temporal resolution allowed for the broadening of the identification range to 15–95 days. A 15–95 day band-pass filter was performed by subtracting the time series obtained from two low-pass filters, consisting of median averages over running windows of 15 and 95 days, particularly suited for time series with missing data. Seasonal harmonics (120 days, semi-annual and annual) have been previously removed. The 15–95 day filter was used to derive intraseasonal variations of sea level (SLAi), significant wave heights at breaking (Hsi), and depth-contours (Xi) in beach profile evolution.

Fifteen intraseasonal sea level events (SLAi) have been identified along the 3.5 years' time series (figure 3). About 80% of the intraseasonal events that have been identified are associated with coastal trapped waves propagating westward (for details, see appendix B) with an average speed of 1.1 m s^{-1} computed manually, an average period of 59 days and an average amplitude of 6.6 cm.

5. Intraseasonal beach response

The correlation computed between the intraseasonal wave energy (figure 3(c)) and the associated intraseasonal depth contours variations suggests that the intensity of the wave's action on beach response is linearly dependent on sea level at intraseasonal scale. The highest correlation values ($r = -0.73$ and $r = +0.41$ for the upper beach and terrace, respectively), computed significant at 95% confidence level (p-value $< 10^{-4}$ and p-value $= 0.0097$, respectively), are observed when intraseasonal sea level is high (SLAi $> +0.02$ m). Correlations values decrease with intraseasonal sea level to reach the lowest values ($r = -0.05$ and $r = -0.09$) when intraseasonal sea level is low (SLAi < -0.02 m). This observation suggests that the combination of waves and sea level events would result in a modulation of wave action on the beach at intraseasonal scale as a function of intraseasonal sea level and thus a response of the beach profile to intraseasonal sea level. However, this dependence remains less marked on the terrace, as the highest correlation value obtained ($r = +0.41$) explains only 17% of the variance.

In order to understand the action of SLAi, morphological changes on beach profile were measured during SLAi events. Figure 4 presents the relationship between changes in intraseasonal sea level events (ΔSLAi) and associated morphological changes (ΔXi). Correlations between ΔSLAi and ΔXi were computed statistically significant at the 95% confidence level. Interestingly, the changes in SLAi are significantly related to changes on the upper beach ($r = -0.81$), even if less related to changes on the terrace ($r = +0.49$). Correlation values suggest that morphological changes at the intraseasonal scale are not only due to wave conditions and coastal currents, but also to sea level variations. Waves and coastal currents (e.g. rip currents) may explain the dispersion of the events observed with the error bars in figure 4.

These observations are confirmed by combining all the intraseasonal events (figure 5). This consists on median-averaging all the considered events, previously interpolated on the same number of samples. The observed impact of the SLAi ensemble event is the deformation of the beach profile with a rise or fall in the sea level. A phase shift of about 9 days is observed between the response of the terrace and the SLAi event. The correlations between the SLAi event and the beach changes are −0.93 and 0.76, respectively for the upper beach and the terrace (considering a 9-day lag for the terrace response). Therefore, two phases can be clearly identified

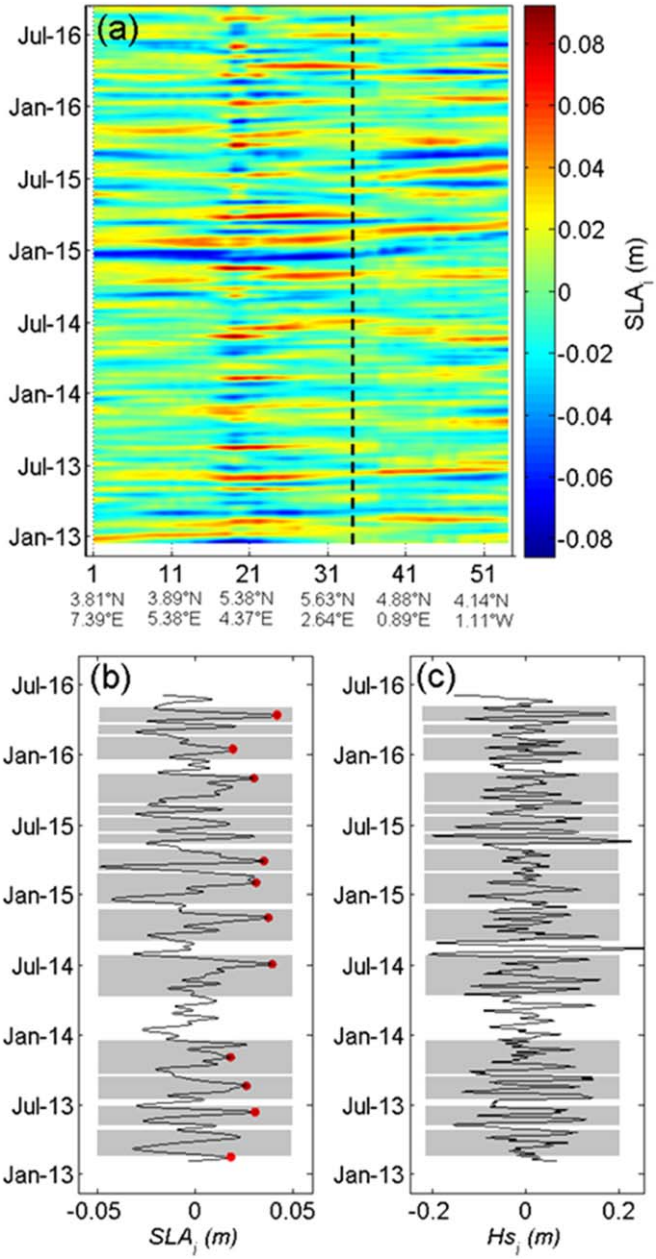

Figure 3. Intraseasonal variations in sea level anomalies (SLAi) and wave height (Hsi) at breaking: (a) Longitude/latitude-time diagram of intraseasonal anomalies, following nodes on the track in figure 1(a). Dashed black line corresponds to node 34, near Grand Popo town, and the corresponding intraseasonal sea level and wave height variations are shown in (b) and (c), respectively. Shaded gray areas stand for considered intraseasonal sea level events. Red points stand for detected propagating peaks of intraseasonal sea levels, with an average speed of 1.1 m s^{-1}.

(figure 5(c)). During a 30-day period of rising sea level, the upper beach is eroded. On the terrace, the concurrent seaward migration of the 1 to 2-m depth-contour lines indicates terrace widening and therefore suggests offshore sand transport. During a 30-day period of lowering sea level, observations indicate upper beach accretion and deeper terrace and therefore suggest onshore sand transport from the terrace to the upper beach. The 9-day lag could represented the time required for sediment to move from the upper beach to the terrace and vice versa. On average, a 7-cm change in sea level leads to nearly 2 m of horizontal terrace deformation as shown in figure 5(d).

6. Influence of intraseasonal sea level variations on beach morphology

Our observations show a deformation of the beach profile with varying intraseasonal sea level, rather than a translation of the profile, corresponding to a retreat of the upper beach and a terrace widening during a high event. The predominant control of wave events on the beach is found to be higher during high sea levels than

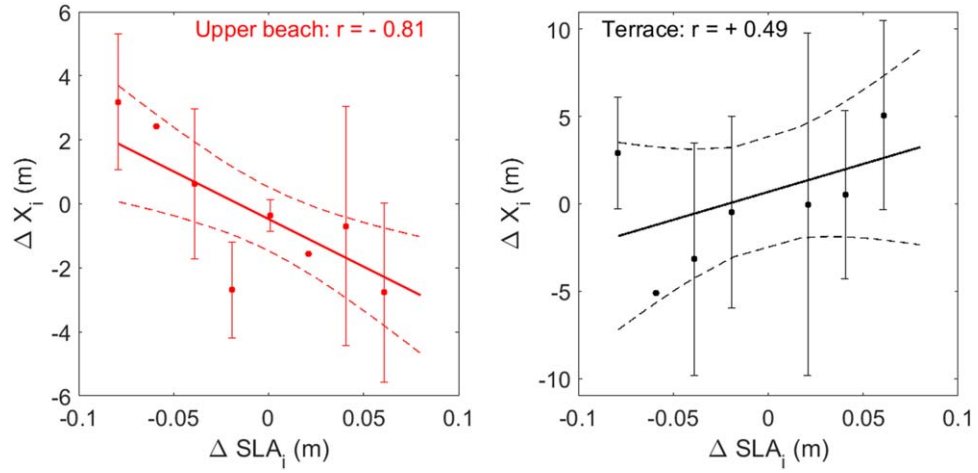

Figure 4. Intraseasonal sea level (ΔSLAi) and corresponding morphological (ΔXi) changes during SLAi events. Solid lines are linear regression and dashed lines indicate the 95% confidence levels. Dots stand for changes (ΔSLAi and ΔXi) computed between the end and the beginning of the ascending and descending phases of an SLAi event, and averaged (using median) over a 0.02 m-window interval on the x-axis, for upper beach and terrace, respectively. Error bars indicate the dispersion of events within the window.

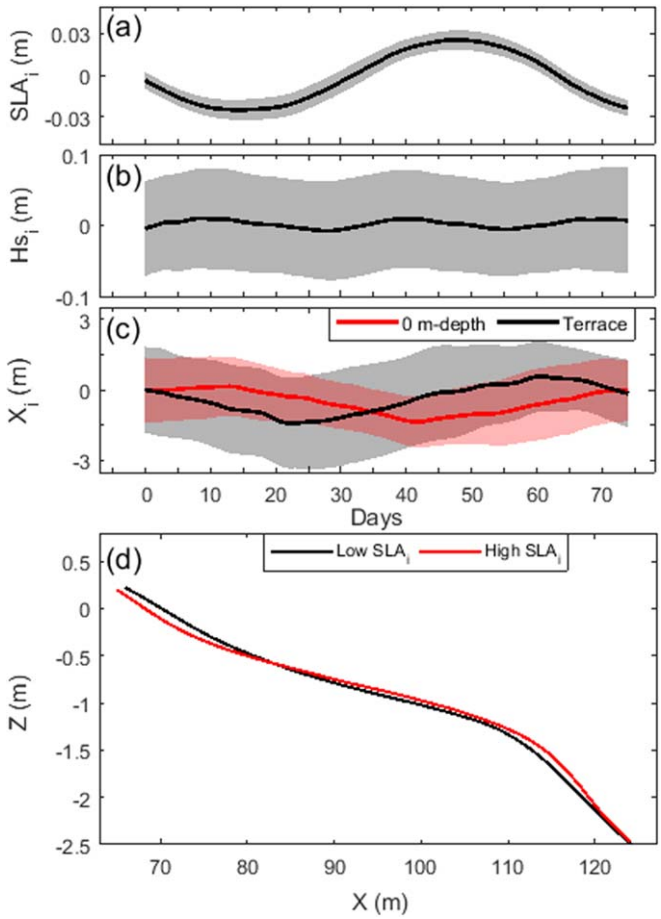

Figure 5. Ensemble-averaged evolution over intraseasonal events and morphological changes with shaded areas representing one standard deviation: (a) Sea level SLAi, (b) wave height Hsi, (c) depth-contours (Xi) corresponding to upper beach (blue) and terrace (black), (d) Mean profiles for high (red) and low (black) sea levels during a 7-cm mean change in SLAi.

during low levels. This suggests that sea level variations modulate the magnitude of wave action on the beach. Some studies (Miles and Russel 2004, Almeida *et al* 2017) have already highlighted this specific behavior at terraced beaches when looking at shorter intra-tidal variations. The combination of a two-slope beach and varying tidal heights brings a complex situation where the separate sections of the beach respond as quite

different systems (Huntley and Bowen 1975), despite being exposed to the same offshore waves. The two sections do interact depending on the water depth on the terrace, with a shallow terrace breaking incident waves as spilling breakers before they reach the upper part of the beach (Miles and Russel 2004). It is hypothesized that during high sea levels, higher average water level across the entire terrace results in less depth-induced breaking wave energy dissipation and, in turn, more energetic waves at the beach face. This can drive more pronounced upper beach erosion, with sediment further supplying the outer edge of the terrace, resulting in terrace enlargement. This explanation needs to be tested and validated, given the complex interplay and the feedback between cross-shore sediment transport driven by undertow and wave non-linearities. Field measurements of sand transport using similar approach to Miles and Russel (2004) would provide more insight into sediment fluxes between the upper beach and the terrace. However, maintaining such measurements during 10 s days is challenging. State-of-the-art beach profile process-based models (e.g. Ruessink *et al* 2007, Kuriyama 2012, Walstra *et al* 2012, Dubarbier *et al* 2015) have the potential to address the underlying mechanisms, but this remains out of scope of the present study. This issue will be addressed in a future modelling study.

Multi-scale coastal evolution, due to sea level variations, remains poorly known. As noted earlier, only the sea-level rise is well known to lead to a recession of the shoreline at decadal to centenary scales (Passeri *et al* 2014, Le Cozannet *et al* 2019). At shorter time scales, from hours to years, sea level variations also influence the beach variability. But, there is still very little literature on their impact on the coast, especially since waves and tide were traditionally the only two forcings studied to understand beach dynamics at open coasts. In this work, focus has been given to intraseasonal sea level variations, which affect the entire African tropical coast (Polo *et al* 2008). And the wave energy was observed to be modulated by sea level variations. A recent study (Segura *et al* 2018) has investigated the role of water level at a reef-fringed beach, which is modulated by wave heights, wave set-up and wave-driven flows, due to saturation of the surf zone and the corresponding variability in depth-limited wave breaking (Thornton and Guza 1982). The beach response was shown to be primarily dictated by the variability in subtidal water levels at seasonal scale, comparatively to wave energy (Segura *et al* 2018). Although these studies were conducted on sites with very different characteristics (sandy beach and reef-fringed beach), the results suggest that the multi-temporal coupling between water level and wave energy must be considered to understand beach dynamics. Such studies should also be investigated on various sites, including coasts where meteotsunamis have been reported (Carvajal *et al* 2017). This requires the development of tools and devices for measuring and modelling coastal dynamics at different time and spatial scales.

7. Conclusions

This study investigated beach changes to intraseasonal sea level variations using 3.5 years of daily video-derived beach profiles and altimetry. The results reveal that sea level variations of order tens of cm at intraseasonal scale drive beach changes: the beach response is not a simple translation of the profile from sea level but a deformation of the profile. As a hypothesis, the intraseasonal sea levels modulate wave action on the beach, inducing erosion of the upper beach and transfer of sediments to the outer part of the terrace during high sea levels. The underlying mechanisms will be tested and validated using detailed process-based beach profile models. The coupling between wave energy and sea level variations could be the key mechanism for multi-temporal understanding of the beach dynamics at open coasts, in particular in the context of current changes of wave regimes and sea level with climate changes. However, further works are needed to investigate the variability of the total sea level at the coast and the associated morphological changes.

Acknowledgments

This publication was made possible through the support provided by the IRD (French Institute of Research for Development). Many thanks to Zacharie Sohou, Gaël Alory, Remy Chuchla and Yves du Penhoat for their technical support in maintaining the video system of Grand Popo, Benin. The Grand Popo experiment was supported by the French INSU/CNRS EC2CO-LEFE/IRD, IRHOB, and UNESCO Co-Chair ICMPA/UAC. We are indebted to the 'Forces Navales' of Benin at Grand Popo for their logistic support during the field experiment and for allowing the installation of the permanent video system on the semaphore. Thanks are due to Habib Dieng for downloading COPERNICUS SSALTO/DUACS products (http://marine.copernicus.eu/services-portfolio/access-to-products). Gridded bathymetry data were downloaded from GEBCO website (www.gebco.net).

ORCID iDs

G O Abessolo https://orcid.org/0000-0001-7724-5805
R Almar https://orcid.org/0000-0001-5842-658X

References

Aarninkhof S G J, Turner I L, Dronkers D T, Caljouw M and Nipius L 2003 A video-base technique for mapping intertidal beach bathymetry *Coastal Eng.* **49** 275–89
Abessolo G O *et al* 2016 Potential of video cameras in assessing event and seasonal coastline behaviour: Grand Popo, Benin (Gulf of Guinea) *J. Coast. Res.* **75** 442–6
Abessolo G O *et al* 2017a Development of a West and Central Africa regional video camera network to monitor coastal response to multiscale ocean forcing *Proc. of Coastal Dynamics (11–16 June 2017) (Helsing)r, Danemark1540–50*
Abessolo G O, Almar R, Castelle B, Testut L, Leger F, Sohou Z, Bonou F, Bergsma E, Meyssignac B and Larson M 2019 Sea level at the coast from video-sensed waves: comparison to tidal gauges and satellite altimetry *J. Atmos. Oceanic Technol.* **36** 1591–603
Abessolo G O, Bonou F, Tomety F S, Du Penhoat Y, Perret C, Degbe C G E and Almar R 2017b Beach response to wave forcing from event to inter-annual time scales at Grand Popo, Bénin (Gulf of Guinea) *Water* **9** 447
Almar R *et al* 2014 The Grand Popo beach 2013 experiment, Benin, West Africa: from short timescale processes to their integrated impact over long-term coastal evolution *J. Coast. Res.* **70** 651–6
Almar R, Kestenare E, Reyns J, Jouanno J, Anthony E J, Laibi R, Hemer M, Du Penhoat Y and Ranasinghe R 2015 Response of the Bight of Benin (Gulf of Guinea, West Africa) coastline to anthropogenic and natural forcing: I. Wave climate variability and impacts on the longshore sediment transport *Cont. Shelf Res.* **110** 48–59
Almar R, Ranasinghe R, Senechal N, Bonneton P, Roelvink D, Bryan K R, Marieu V and Parisot J P 2012 Video-based detection of shorelines at complex meso–macro tidal beaches *J. Coast. Res.* **28** 1040–8
Almar R, Senechal N, Bonneton P and Roelvink J A 2008 Wave celerity from video imaging: a new method *Proceedings of the 31st International Conference Coastal Engineering* **1** 661–73
Almeida l P, Almar R, Blenkinsopp C, Martins K, Benshila R and Daly C 2017 Swash dynamics of a sandy beach with low tide terrace *Proc. of Coastal Dynamics* 11–16 June 2017) *(Helsing)r, Danemarkpp 258–67*
Aman A, Testut L, Woodworth P, Aarup T and Dixon D 2007 Seasonal sea level variability in the Gulf of Guinea from altimetry and tide gauge *Rev. Ivoir. Sci. Technol.* **9** 105–18
Amarouche L, Thibaut P, Zanife O, Dumont J-P, Vincent P and Steunou N 2004 Improving the Jason-1 ground retracking to better account for attitude effects *Mar. Geod.* **27** 171–97
Anthony E, Almar R, Besset M, Reyns J, Laibi R, Ranasinghe R, Abessolo Ondoa G and Vacchi M 2019 Response of the Bight of Benin (Gulf of Guinea, West Africa) coastline to anthropogenic and natural forcing: II. Sources and patterns of sediment supply, sediment cells, and recent shoreline change *Cont. Shelf Res.* **173** 93–103
Arbic B K, Scott R B, Chelton D B, Richman J G and Shriver J F 2012 Effects on stencil width on surface ocean geostrophic velocity and vorticity estimation from gridded satellite altimeter data *J. Geophys. Res.* **117** C03029
Atkinson A L, Baldock T E, Birrien F, Callaghan D P, Nielson P, Beuzen T, Turner I L, Blenkinsopp D P and Ranasinghe R 2018 Laboratory investigation of the Bruun Rule and beach response to sea level rise *Coastal Eng.* **136** 183–202
Bruun P 1954 Coast erosion and the development of beach profiles. Technical Memorandum 44. Beach Erosion Board, Corps of Engineers, 82 pp
Bruun P 1962 Sea-level rise as a cause of shore erosion *J. Waterway. Harbours Div.* **88** 117–30
Bruun P 1983 Review of conditions for uses of the Bruun rule of erosion *Coast. Eng.* **7** 77–89
Bruun P 1988 The Bruun rule of erosion by sea-level rise: a discussion of large-scale two- and three-dimensional usages *J. Coast. Res.* **4** 627–48 (https://jstor.org/stable/4297466)
Carvajal M, Contreras-Lopez M, Winckler P and Sepulveda I 2017 Meteotsunamis occurring along the Southwest Coast of South America during an intense storm *Pure Appl. Geophys.* **174** 3313–23
Le Cozannet G, Bulteau T, Castelle B, Ranasinghe R, Woppelmann G, Rohmer J, Bernon N, Idier D, Louisor J and Salas-y-Mélia D 2019 Quantify uncertainties of sandy shoreline change projections as sea level rises *Sci. Rep.* **9** 42
Le Cozannet G, Oliveros C, Castelle B, Garcin M, Idier D, Pedreros R and Rohmer J 2016 Uncertainties in sandy shorelines evolution under the bruun rule assumption *Frontiers in Marine Science* **3** 49
De Coëtlogon G, Janicot S and Lazar A 2010 Intraseasonal variability of the ocean—atmosphere coupling in the Gulf of Guinea during boreal spring and summer *Q. J. R. Meteorol. Soc.* **136** 426–41
Dean R G and Houston J R 2016 Determining shoreline response to sea level rise *Coastal Eng.* **114** 1–8
Ding H, Keenlyside N S and Latif M 2009 Seasonal cycle in the upper equatorial Atlantic Ocean *J. Geophys. Res.* **114** c09016
Ding Y, Bao X, Yao Z, Song D, Song J, Gao J and Li J 2018 Effect of coastal-trapped waves on the synoptic variations of the Yellow Sea warm current during winter *Cont. Shelf Res.* **167** 14–31
Dubarbier B, Castelle B, Marieu V and Ruessink G 2015 Process-based modelling of cross-shore sandbar behavior *Coastal Eng.* **95** 35–50
Echevin V, Albert A, Lévy M, Graco M, Aumont O, Piétri A and Garric G 2014 Intraseasonal variability of nearshore productivity in the Northern Humboldt Current System: the role of coastal trapped waves *Cont. Shelf Res.* **73** 14–30
Ezer T 2016 Can the Gulf Stream induce coherent short-term fluctuations in sea level along the US East Coast? A modeling study *Ocean Dyn.* **66** 207–20
Feng M, Meyers G, Pearce A and Wijffels S 2003 Annual and interannual variations of the Leewin Current at 32 S *J. Geophys. Res.* **108** 3355
Giardino *et al* 2018 A quantitative assessment of human interventions and climate change on the West African sediment budget *Ocean Coastal Management* **156** 249–65
Holland K T and Holman R A 1993 The statistical distribution of swash maxima on natural beaches *J. Geophys. Res.* **98** 10271–8
Holland K T, Holman R A, Lippmann T C, Stanley J and Plant N 1997 Practical use of video imagery in near-shore oceanographic field studies *IEEE J. Oceanic Engineering* **22** 81–92
Huntley D A and Bowen A J 1975 Comparison of the hydrodynamics of steep and shallow beaches ed J Hails and A Carr *Nearshore Sediment Dynamics and Sedimentation* (London: Wiley) pp 69–109

Jouanno J, Marin F, du Penhoat Y and Molines J-M 2013 Intraseasonal modulation of the surface cooling in the Gulf of Guinea *J. Phys. Oceanogr.* **43** 382–401
Kim J-K, Choi B-J and Lee S-H 2018 Non-seasonal sea level variations in the Korea Strait and regional atmospheric conditions *J. Coast. Res.* **85** 581–5
Komar P D, Allan J C and Ruggiero P 2011 Sea level variations along the U.S. Pacific Northwest coast: tectonic and climate controls *J. Coast. Res.* **27** 808–23 West Palm Beach (Florida), ISSN 0749-0208 (https://doi.org/10.2112/JCOASTRES-D-10-00116.1)
Komar P D and Enfield D B 1987 Short-term sea-level changes and coastal erosion Book chapter, https://doi.org/10.2110/pec.87.41.0017
Kuriyama Y 2012 Process-based one-dimensional model for cyclic longshore bar evolution *Coastal Eng.* 48–61
Larson M, Hoan L X and Hanson H 2010 A direct formula to compute wave properties at incipient breaking *J. Waterw. Port Coastal Ocean Eng.* **136** 119–22
Leonard M, Westra S, Phatak A, Lambert M, van den Hurk B, McInnes K, Risbey J, Schuster S, Jakob D and Stafford-Smith M 2014 A compound event framework for understanding extreme impacts *Wiley Interdiscip Rev. Clim. Chang.* **5** 113–28
McInnes K L *et al* 2016 Natural hazards in Australia: sea level and coastal extremes *Clim. Change* **139** 69–83
Melet A, Almar R and Meyssignac B 2016 What dominates sea level at the coast: a case study for the Gulf of Guinea *Ocean Dyn.* **66** 623–36
Melet A, Meyssignac B, Almar R and Le Cozannet G 2018 Under-estimated wave contribution to coastal sea-level rise *Nat. Clim. Change* (https://doi.org/10.1038/s41558-018-0088-y)
Miles J R and Russel P E 2004 Dynamics of a reflective beach with a low tide terrace *Cont. Shelf Res.* **24** 1219–47
Nicholls R J and Cazenave A 2010 Sea-level rise and its impact on coastal zones *Science* **328** 1517–20
Passeri D L, Hagen S C and Irish J L 2014 Comparison of shoreline change rates along the south Atlantic Bight and northern Gulf of Mexico coasts for better evaluation of future shoreline positions under sea level rise *J. Coast. Res.* **68** 20–6
Pattiaratchi C and Eliot M 2009 Sea level variability in south-west Australia: from hours to decades *31st Int. Conf. onCoastal Engineering* (https://doi.org/10.1142/9789814277426_0099)
Polo I, Lazar A, Rodriguez-Fonseca B and Arnault S 2008 Oceanic Kelvin waves and tropical Atlantic intraseasonal variability: I. Kelvin wave characterization *J. Geophys. Res.* **113** C07009
Pujol M-I, Faugère Y, Taburet G, Dupuy S, Pelloquin C, Ablain M and Picot N 2016 DUACS DT2014: the new multimission altimeter data set reprocessed over 20 years *Ocean Sci.* **12** 1067–90
Ranasinghe R 2016 Assessing climate change impacts on open sandy coasts: a review *Earth-Sci. Rev.* **160** 320–32
Ranasinghe R, Callaghan D and Stive M J F 2012 Estimating coastal recession due to sea level rise: beyond the bruun rule *Clim. Change* **110** 561–74
Rosati J, Dean R and Walton T 2013 The Modified bruun rule extended for landward transport *Mar. Geol.* **340** 71–81
Rueda A *et al* 2017 A global classification of coastal flood hazard climates associated with large-scale oceanographic forcing *Sci. Rep.* **7** 5038
Ruessink B G, Kuriyama Y, Reniers A J H M, Roelvink J A and Walstra D J R 2007 Modeling cross-shore sandbar behavior on the timescale of weeks *J. Geophys. Res.* **12** F03010
Santoro P E, Fossati M and Piedra-Cueva I 2013 Study of the meteorological tide in the Río de la Plata *Cont. Shelf Res.* **60** 51–63
Segura L E, Hansen J E and Lowe R J 2018 Seasonal shoreline variability induced by subtidal water level fluctuations at reef-fringed beaches *Journal of Geophysical Research: Earth Surface* **123** 433–47
Shand T, Shand R, Reinen-Hamill R, Carley J and Cox R 2013 A review of shoreline response models to changes in sea level *Coasts and Ports Australiasian Conf. (Sydney, 11–13 September)*
Slangen A B *et al* 2017 Evaluating model simulations of twentieth-century sea level rise: I. Global mean sea level change *J. Clim.* **30** 8539–63
Sterl A and Caires S 2005 Climatology, variability and extrema of ocean waves- the web-based KNMI/ERA-40 Wave Atlas *Int. J. Climatol.* **25** 963–77
Stive M J F 2004 How important is global warming for coastal erosion? *Climate Change* **64** 27–39
Stive M J F, Aarninkhof S G J, Hamm L, Hanson H, Larson M, Wijnberg K M, Nicholls R J and Capobianco M 2002 Variability of shore and shoreline evolution *Coastal Eng.* **47** 211–35
Thornton E B and Guza R T 1982 Energy saturation and pase speeds measured on a natural beach *J. Geophys. Res.* **87** 9499–508
Tran N, Labroue S, Philipps S, Bronner E and Picot N 2010 Overview and update of the sea state bias corrections for the Jason-2, Jason-1 and TOPEX missions *Mar. Geod.* **33** 348–62
Ubelmann C, Ballarotta M, Faugere Y, Rogé M, Morrow R and Dibarboure G 2017 Upcoming high-resolution regional products of sea level anomaly from dynamic interpolation *OSTS* (https://meetings.aviso.altimetry.fr/fileadmin/user_upload/tx_ausyclsseminar/files/Poster_DI_OSTST2017.pdf)
Ubelmann C, Klein P and Fu L-L 2015 Dynamic interpolation of sea surface height and potential applications for future high-resolution altimetry mapping *J. Atmos. Oceanic Technol.* **32** 177–84
Vialard J, Shenoi S S C, McCreary J P, Shankar D, Durand F, Fernando V and Shetye S R 2009 Intraseasonal response of the northern Indian Ocean coastal waveguide to the Madden-Julian Oscillation *Geophys. Res. Lett.* **36** L14606
Walstra D J R, Reniers A J H M, Ranasinghe R, Roelvink J A and Ruessink B G 2012 On bar growth and decay during interannual net offshore migration *Coastal Eng.* **60** 190–200
Wingham D J, Francis C R, Baker S, Bouzinac C, Brockley D, Cullen R and de Chateau-Thierry P 2006 CryoSat: a mission to determine the fluctuations in Earth's land and marine ice fields *Adv. Space Res.* **37** 841–71
Wright L D and Short A D 1984 Morphodynamic variability of surf zones and beaches: a synthesis *Mar. Geol.* **56** 93–118
Zhang K, Douglas B C and Leatherman S P 2004 Global warming and coastal erosion *Climate Change* **64** 41–8